Essential Readings in Light Metals: Alumina and Bauxite.
Edited by Don Donaldson and Benny E. Raahauge.

DYNAMIC MODELING OF YIELD AND PARTICLE SIZE DISTRIBUTION IN CONTINUOUS BAYER PRECIPITATION

Jerry L. Stephenson
Aluminum Company of America
Alcoa Technical Center, 100 Technical Drive, Alcoa Center, PA 15069

Chris Kapraun
Alcoa Alumina & Chemicals, L.L.C.
Point Comfort Operations, State Highway 35, Point Comfort, TX 77978

Abstract

Process engineers at Alcoa's Point Comfort refinery are using a dynamic model of the Bayer precipitation area to evaluate options in operating strategies. The dynamic model, a joint development effort between Point Comfort and the Alcoa Technical Center, predicts process yields, particle size distributions and occluded soda levels for various flowsheet configurations of the precipitation and classification circuit. In addition to rigorous heat, material and particle population balances, the model includes mechanistic kinetic expressions for particle growth and agglomeration and semi-empirical kinetics for nucleation and attrition. The kinetic parameters have been tuned to Point Comfort's operating data, with excellent matches between the model results and plant data. The model is written for the ACSL dynamic simulation program with specifically developed input/output graphical user interfaces to provide a user-friendly tool. Features such as a seed charge controller enhance the model's usefulness for evaluating operating conditions and process control approaches.

Introduction

To a large extent the Bayer precipitation area governs product yield and many product quality characteristics such as the particle size distribution and impurity levels. Managing the operations of the precipitation circuit to optimize its performance continues to be one of the most challenging aspects of running a Bayer bauxite refinery. To help plant process engineers make operating decisions for the precipitation circuit, Alcoa initiated the development of a dynamic flowsheet model of the precipitation, classification and seed recycle area. Combining rigorous heat and material balance equations with mechanistic kinetic expressions for the particle population balances has created a tool that can predict process behavior for process changes before implementing them in the actual plant. Having the capability to model transient behavior as well as the steady-state conditions permits evaluation of process control strategies.

This simulator provides a quantitative analysis of the entire precipitation system by modeling the dynamics in each vessel in a cascade precipitation row and its associated classification bank. The classification portion estimates the partition of the various alumina hydrate particle sizes between the overflows and underflows of each classifier.

Background

Many parts of the Bayer process have been studied and modeled with the goal of understanding and improving process performance. Comprehensive steady-state models of both individual operating areas and the entire Bayer liquor circuit have been developed using the ASPEN flowsheet simulator by Langa, et al. [1]. Such steady-state models are useful for establishing controller setpoints for optimal process performance as demonstrated by Stephenson [2]. The PRECIP model by Swansiger [3] is a notable example of a steady state model of the precipitation area concentrating on the crystallization growth rate expression and the overall heat and material balances.

Dynamic process models have the added advantage of simulating process transients for evaluating process controllers in addition to their capability of calculating the steady-state solution. Chapman, Winter, and Barton [4] published a dynamic model of a simplified precipitation circuit using the SPEEDUP simulator. Representation of the particle population balances in this simulation was limited to the effects of crystal growth and the flows in and out of units. Crama and Visser [5] published a comprehensive dynamic model for precipitation and classification flowsheets with the particle population balances extended to include agglomeration and nucleation.

The present Alcoa model combines flexible flowsheet configuration, rigorous heat and material balances, thermophysical property routines specific to Bayer liquors, and a complete particle population balance representation in a dynamic simulator. An isothermal run option allows specification of temperatures in the precipitator and classification stages which suppresses the heat balance equations. This option is especially useful for the cases where the heat transfer coefficients for ambient heat loss have not been evaluated. Additional controller features permit accurate modeling of the plant operations and prediction of process behavior for alternate operating conditions. Recent participation by plant process engineers has accelerated the model development to make it more accessible and useful to plant personnel.

Model structure

The precipitation/classification model is structured as a dynamic flowsheet model with the vessels represented as dynamic, perfectly-stirred stages. Each precipitator is modeled as a single stage, while each classifier vessel is modeled as two stages to simulate the different dynamics of the overflow and underflow regions. Flows between vessels are represented by stream vectors with an information structure similar to sequential modular simulators. The values in these vectors include the total mass flow, mass fractions of the individual components, particle size distribution, temperature, specific enthalpy, and density.

Through the input data file, the user specifies the specific flowsheet configuration to be simulated. Currently up to seven cascade precipitator tanks can be selected as shown in Figure 1. Minor coding could increase the allowable number of tanks if needed to simulate other plants. Classification consists of either two or three thickener vessels to generate recycle seed as well as the feed to the hi-tank where product is transferred

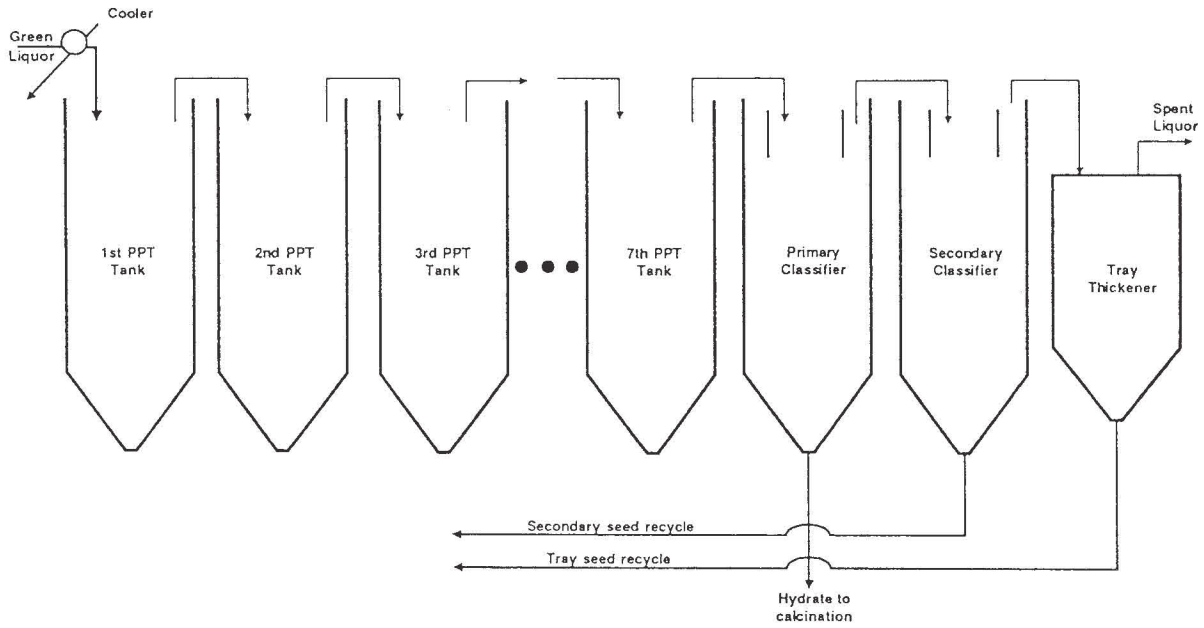

Figure 1. Continuous Precipitation Row

to the final washing and filtering prior to calcination (see Figure 2). Complete seeding flexibility is provided in that each precipitator can be seeded with all three types of recycled seed. The model can be run in either an open-loop mode, in which the seed stream flows and compositions are specified by the input data file, or in a closed-loop mode in which the seed streams are determined by the simulation of the classification bank

Components

For ease of use, the model uses typical Bayer plant terminology, such as Al2O3 g/l at standard conditions, for inputs and outputs. However, the model uses nine specific chemical components for all internal calculations. Liquid phase components include water, soda in solution, sodium aluminate, sodium carbonate, sodium sulfate, sodium chloride and dissolved organics. Solid components include alumina trihydrate (gibbsite) and occluded soda. With these components the gibbsite precipitation reaction is written as

$$(NaAlO_2)_2 + 3\,H_2O \Leftrightarrow Al_2O_3{*}3H_2O\,(s) + Na_2O \qquad (1)$$

The alumina trihyrate particle population (size distribution) is discretized into forty-five size increments. The particles are assumed to be spherical with a diameter range of 0 to 300 microns. The characteristic particle diameters of the size increments are more closely spaced at the fine end of the size distribution and increase as a geometric progression.

Vessel representation

The dynamic stage model used to represent vessels contains the dynamic heat, mass, and population balance equations. The gibbsite precipitation reaction is included as well as the reaction for soda occluded in the gibbsite particles. For the population balance equations, the stage model calls the appropriate subroutines for crystal growth, agglomeration, nucleation, and attrition. These topics are discussed in more detail in another section of this paper. The stage model also calls the appropriate thermophysical property correlations for density and enthalpy for the current stage composition. Both the density and enthalpy correlations were developed specifically for Bayer liquors by Langa [6].

In the Point Comfort model, the stage models adhere to all CSTR assumptions which match typical operating practices of minimal short circuiting and no solids retention. Results to date have shown that the model performance ignoring incomplete mixing in the tanks has been adequate for Point Comfort's operations. A newer version of the model includes solids retention to expand its applicability to other Alcoa refineries.

Particle Population Balances

The key to success in precipitation modeling is handling the dynamic population balances. Randolph and Larson [7] presented the particle population balance for a unit system volume without any flow in or out of the system as

$$\frac{\partial n}{\partial t} + \frac{\partial (G_1 n)}{\partial L} = B - D \qquad (2)$$

where G_1 is the linear growth rate and n is the number density of particles, the number of particles in size increment L to $L+\partial L$ per unit volume of suspension divided by ∂L. The growth term accounts for particles growing into or out of the size increment. The birth (B) and death (D) terms account for the creation and removal of particles in the size increment by agglomeration, attrition, or nucleation (smallest size

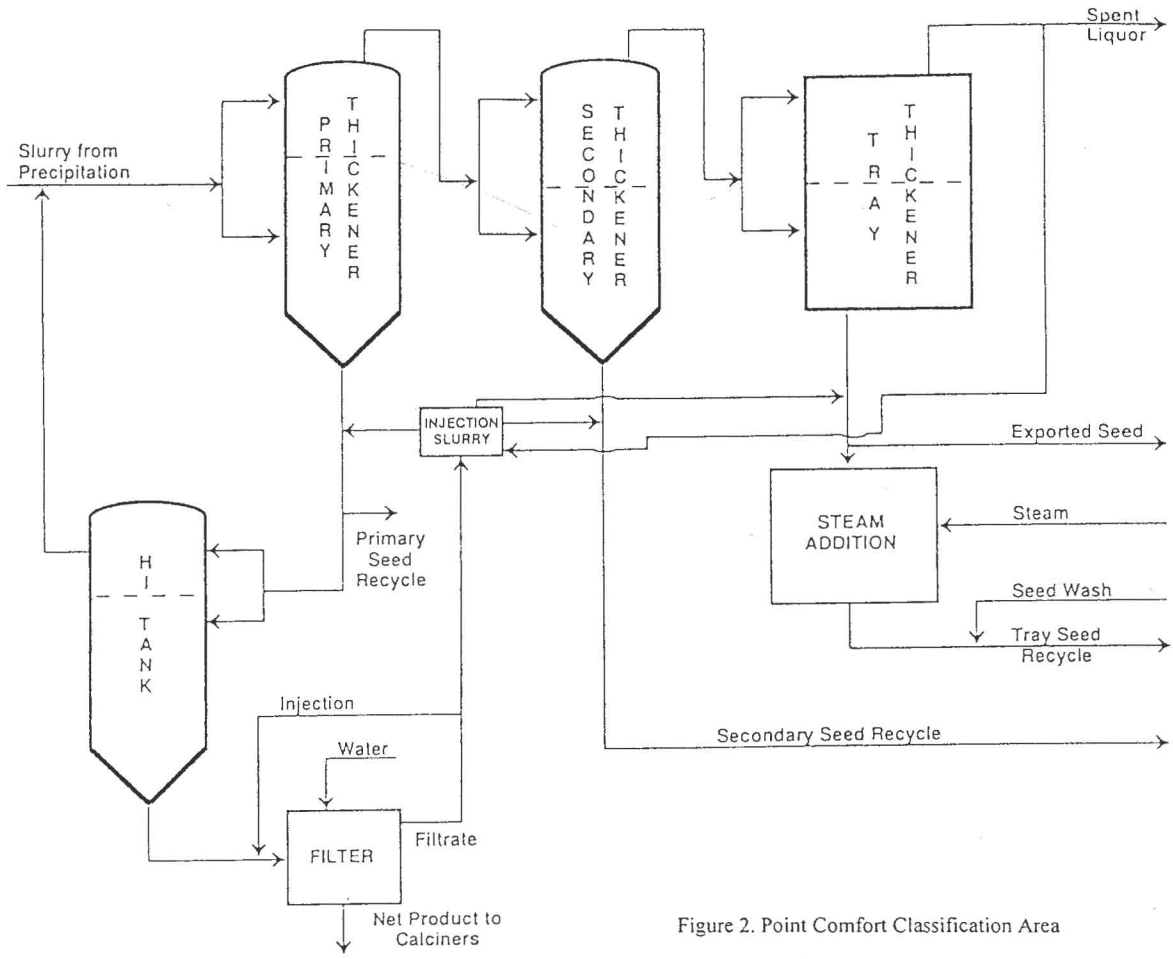

Figure 2. Point Comfort Classification Area

increment only). In the precipitation model, terms for the flows of particle in and out of the system must also be included in the population balance equations.

Crystal Growth

By the mechanism of crystal growth dissolved alumina hydrate transfers from the aqueous phase to the solid phase, depositing on the surface of existing particles. Thus the growth rate determines the overall liquor/solid mass balance. Growth also impacts the particle population balance because particles will increase in diameter in accordance with the McCabe law [8] of a constant linear growth rate (deposition of a layer of uniform thickness on the particle surface) which is independent of particle diameter.

From the work of Scott [9] and King [10], the crystal growth rate in gibbsite precipitation has been shown to depend on three factors: the supersaturation of sodium aluminate in solution, the temperature, and the solid surface area available for reaction. An Arrhenius function describes the temperature dependency, making the growth rate expression

$$G = k_0 e^{-\frac{E_A}{RT}} \left[\frac{A - A^*}{FC} \right]^2 \qquad (3)$$

where

G = Specific growth rate, g/hr/m^2
k_o = Kinetic coefficient
E_A = Activation energy
R = Ideal gas constant
T = Temperature
FC = Free caustic concentration
A = Sodium aluminate concentration
A* = Sodium aluminate solubility at equilibrium

This growth rate equation requires an accurate expression for the equilibrium solubility concentration of sodium aluminate in caustic solution. Misra [11] showed that the solubility is a function of temperature and caustic. Swansiger [3] extended Misra's correlation to include empirical terms for the effects of liquor impurities at concentration levels found in Alcoa's refineries. The precipitation model uses this solubility relationship for Point Comfort simulations.

Agglomeration

Agglomeration occurs when two particles collide and "stick" together to form a larger particle. Agglomeration is essential in gibbsite precipitation because it is the only economically feasible method of producing particles with the required size given the extremely slow growth rate. Agglomeration consumes smaller particles and creates larger particles, representing the additive volume of the smaller particles consumed. According to Cornell and Saunders [12], the nature and extent of agglomeration also affect product toughness and hence the ultimate alumina product size distribution through calcination.

Several studies have been directed at finding agglomeration rate expressions to adequately reflect postulated mechanisms and reproduce experimental data. The studies typically postulate the same general form for the agglomeration rate expression that incorporates a probability that two particles of sizes x_i and x_j will collide, a collision efficiency factor that the collision can result in agglomeration, and an alumina supersaturation factor:

$$Ag(x_i, x_j) = \rho(x_i)\rho(x_j)k(x_i, x_j)f(\sigma) \qquad (4)$$

where

- Ag = Rate of agglomeration of particles of size x_i and x_j
- $x_{i/j}$ = Particle representative diameter
- $\rho(x_i)$ = Probability density function for particle with diameter x_i
- $k(x_i,x_j)$ = Agglomeration kernel (collision efficiency factor)
- σ = Alumina supersaturation term

In this equation, the probability of collisions between the two particles is usually set proportional to the product of their respective particle density functions. The agglomeration kernel, $k(x_i,x_j)$, is a function which describes the collision efficiency for particles of the two specific diameters. The kernel typically contains geometric terms related to the probability that the two particles will meet in an orientation suitable for agglomeration. Groeneweg [13] derived a rather complicated agglomeration kernel which results in significantly decreasing efficiencies as the particle diameters increase. Other studies, such as Low's [14], have suggested a simple size independent kernel which resets to zero for particles exceeding a critical diameter, indicating that particles do not agglomerate above a certain size. Ilievski and White [15] contend, however, that the depletion of supersaturation occurring during the batch tests was responsible for this apparent critical diameter. Ilievski et al. [16] evaluated several candidate agglomeration kernels and concluded that a size independent kernel appeared to match the experimental data best.

After initial work with the Groeneweg agglomeration kernel, better agreement with plant data was obtained when the size-independent kernel was inserted. However, the model still predicted a coarse particle bias for some cases. For added flexibility, the following three parameter agglomeration kernel has been used

$$k(x_i, x_j) = \beta_1\left(e^{-\left(\beta_3 x_i + \beta_4 x_i^2\right)}\right)\left(e^{-\left(\beta_3 x_j + \beta_4 x_j^2\right)}\right) \qquad (5)$$

where $\beta_{1,3,4}$ are tuning parameters evaluated for actual data. This equation is used in combination with a Heaviside step function to limit the maximum possible agglomeration diameter. Other forms of the agglomeration kernel will be considered as the understanding of the basic agglomeration mechanism matures.

Several forms of the supersaturation term have been used in the above studies to represent the "cementing" action of crystallization to complete the agglomeration phenomenon. Groeneweg's $f(\sigma)$ is defined as the alumina supersaturation divided by the equilibrium solubility concentration raised to the third power. Ilievski's work suggests that $f(\sigma)$ be the fourth power of the quantity of the supersaturation divided by the total caustic concentration. The present model uses a function of the specific growth rate.

Nucleation

Nucleation is the formation of new, minute particles which replenish the particle count of the system. Particles are continuously lost through agglomeration or product removal. Thus, for efficient operation, nucleation must provide enough particles to maintain the total particle count and provide surface area for continuing growth.

In the Bayer process, two forms of nucleation, primary and secondary, occur. In the process of primary nucleation, new centers for growth are postulated to form spontaneously from the supersaturated liquid itself. Secondary nucleation is the process whereby new growth centers are formed from the surfaces of preexisting particles through abrasion.

A few studies have tried to link concentration, particle size, and temperature to both forms of nucleation. Misra and White [17] noted the lack of quantitative data on nucleation and hypothesized that primary nucleation above is minimal above 75°C because of the high stability of the supersaturated alumina in solution. The precipitation model uses an unpublished correlation by Misra [18] which includes terms for both primary and secondary nucleation. Primary nucleation is a function of temperature and supersaturation while secondary nucleation depends on the solids concentration in the slurry. Simulations indicate that primary nucleation does not contribute many new particles at Point Comfort's typical operating conditions.

Attrition

Personnel in industry have debated the occurrence of attrition in the vessels, pipes or pumps. An attrition function was added to the model to increase flexibility in modeling the particle population balance throughout the entire circuit. The probability that a particle will break was set proportional to its diameter cubed. The relative sizes of the two smaller particles produced during attrition was held constant relative to size of the starting particle. For typical conditions, the attrition function affects the particle size distribution only slightly.

Model Features

Classification

The Point Comfort model includes a dynamic representation of the classification system that is more empirical than the precipitation area. Each classifier, including the hi-tank product transfer vessel, is considered as two stages because of the vast difference in composition and solid concentration in the overflow and underflow region of each vessel. The inlet stream to each classifier is divided into high and low solids stage inlets. The solid particles are partitioned according to the classifier efficiency function proposed by Molerus [19].

$$s_u(x) = l_u + \frac{1 - l_u}{1 + \left(L(x)/L(x_{50})\right)^{-\alpha}} \qquad (6)$$

where

- $s_u(x)$ = Fraction of solids with size x reporting to underflow stage
- l_u = Fraction of liquid reporting to underflow stage
- $L(x)$ = Representative diameter for particle size increment x
- $L(x_{50})$ = Characteristic diameter for specific classifier
- α = Tuning factor to control extent of separation

The parameter values for each classifier are selected on the basis of historical plant data as well as specific sampling campaigns. After partitioning the solids in each size increment, the model logic splits the incoming liquor flow to match a user-specified solids density target for the classifier underflow.

Injection

The model adjusts the injection flow to the underflows of the classifiers to satisfy user specifications of the solids concentrations after slurry injection. The injection slurry is comprised of filtrate from the final product filter prior to calcination plus additional tray thickener overflow if necessary to meet demands.

Net product removal option

By setting the value in the input file, the user can invoke an option whereby the classifier efficiency functions are automatically adjusted so that the exact net production of gibbsite in the entire circuit, minus the amount in the spent liquor return (tray thickener overflow), is removed via the primary thickener and hi-tank as product to the calciner. This option is useful for evaluating different operating scenarios where one can assume that over time the classification vessels will be operated to remove the net production.

Controller for first stage reaction conditions

Many precipitation engineers consider the conditions of the first precipitation stage to be especially crucial to product quality. Point Comfort operates its precipitation units with the goal of achieving a specific growth rate in the first stage of the cascade. Controller logic to achieve such operation through manipulation of the recycle seed flows to the first stage is provided in the model. The model allows several different recipes for the blending of seed types to the first stage to satisfy the specified reaction conditions. The logic to be used in a specific simulation is specified by user input.

Occluded Soda Reaction Rate

The precipitation model allows for inclusion of a kinetic expression for calculating the soda composition of the gibbsite produced. The exact form of the soda precipitation expression is still a subject of debate in the literature. One approach is to formulate the rate of soda deposition in new hydrate is calculated as an extension of the growth phenomenon such as suggested by Ohkawa and co-workers [20]. A corresponding equation for estimating the percent of soda in freshly deposited hydrate is

$$\%Na_2O = ke^{-\frac{E}{RT}}(\sigma)^2 \qquad (7)$$

which has the Arrhenius functionality. The model currently uses an empirical correlation by Ralphe [21] which appears to be valid over a wider range of conditions. His correlation includes effects of the supersaturation as well as the organic carbon.

The dynamic precipitation model represents the occlusion of soda as a function of growth only. Inhomogeneities in occluded soda concentration for different particle sizes are not modeled.

Solution of the dynamic balance equations

The differential equations governing the component mass balances, the overall mass balance, the particle population balances, and the energy balance must be numerically approximated to provide a dynamic solution to the modeled system. To integrate the simultaneous differential equations, the model uses the Advanced Continuous Simulation Language (ACSL) package [22] from Mitchell and Gauthier Associates, Inc. with its fourth order Runge Kutta routine. Evaluations on step-size provided the maximum allowable integration step-size that resulted in an accurate solution. The ACSL package also provides a collection of analytical tools and built-in forcing functions which permit straightforward dynamic adjustment of inlet flows or compositions for dynamic studies. The ACSL code also provides implementation of discrete-time events. This feature enables simulation of typical discrete-time controller designs.

User friendliness features

One of the primary development goals was to make a model which would be consulted regularly by plant process engineers. To reduce the time required to learn how to use the precipitation model, a simplified graphical user interface was developed. This interface uses online documentation and a logical layout to provide for easy use of the model. The interface allows the user to enter the information needed for a simulation by pressing buttons representing portions of the process as shown in Figure 3.

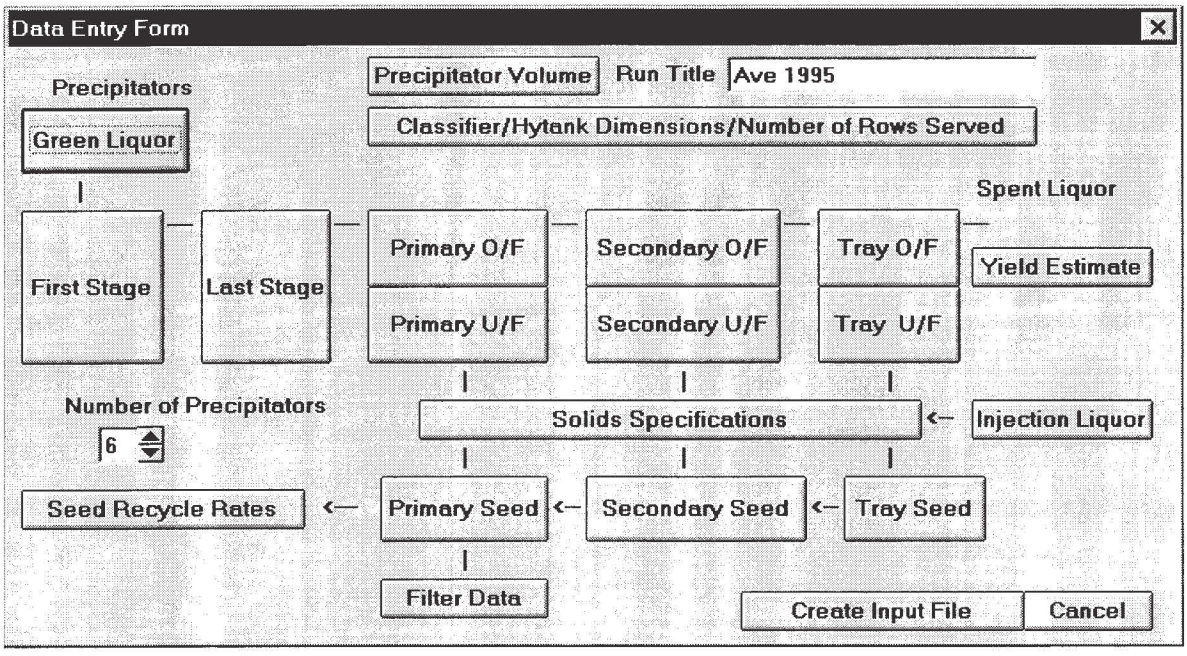

Figure 3. Model Interface

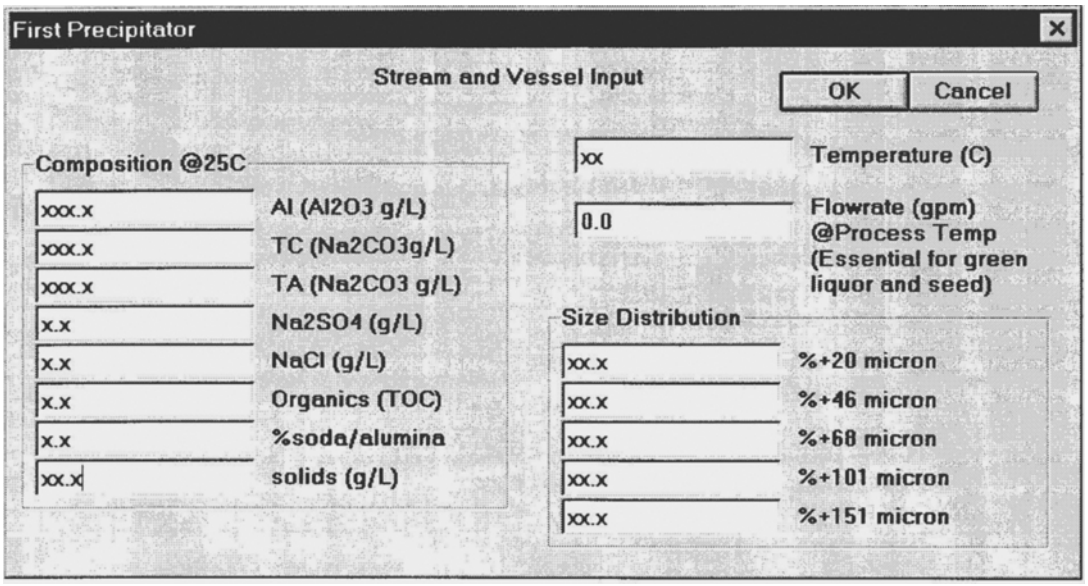

Figure 4. Stream Vector Input Form

The actual data entry forms for vessel and stream data have been simplified to allow the user to enter process data in a format similar to operation summary reports. One of these data forms is presented in Figure 4.

The rest of the user interface allows data input and model execution in simple point and click fashion. The graphical user interface covers most aspects of the program including updating the tuning parameters, entering specifications, creating the input data file, running the model, and formatting the output for display or printing.

Comparison to plant data

To develop confidence in the precipitation model, its predictions were verified against plant operating results. First the kinetic rate parameters in the model were estimated by fitting the model to a year's worth of historic plant data. For these simulations the model was run in the isothermal mode in which the precipitation stage temperatures are specified by the input data file to match plant conditions. Without changing any of the parameter values, the model was then applied to data from other operating periods. Table 1 shows the typical percent errors between the plant data and the model predictions for both the base case used for parameter evaluation and for a subsequent set of monthly operating data. Model verification has also been extended to the full closed loop circuit including classification and seed preparation. With the semi-empirical nature of the classification area, the effort to match plant data becomes more challenging. Table 2 shows typical results for the full closed loop model.

Table 1. Open Loop Results for Precipitation Model

Process Variable	1994 Yearly Percent Error	Apr-95 Percent Error
%+20 Micron in First Precipitator	0.03	0.22
%+20 Micron in Last Precipitator	0.78	0.74
%+68 Micron in First Precipitator	3.38	3.41
%+68 Micron in Last Precipitator	2.04	3.22
%+101 Micron in First Precipitator	1.69	1.64
%+101 Micron in Last Precipitator	4.34	5.41
Total Caustic in First Precipitator (g/L)	0.38	0.23
Total Caustic in Last Precipitator (g/L)	0.21	0.29
A/TC Ratio in First Precipitator	0.95	2.06
A/TC Ratio in Last Precipitator	1.07	1.4
g/L Solids in Last Precipitator	2.13	0.83

Table 2. Predicted and Actual Process Values for Closed Loop Simulation of May 1995 Plant Operations

Variable	Percent Error
%+20 Micron Secondary Seed	1.32
%+20 Micron Tray Seed	3.98
%+68 Micron Secondary Seed	2.67
%+68 Micron Tray Seed	10.38
%+101 Micron Secondary Seed	3.13
%+101 Micron Tray Seed	7.00
%+20 Micron in First Precipitator	0.27
%+20 Micron in Last Precipitator	0.70
%+68 Micron in First Precipitator	9.44
%+68 Micron in Last Precipitator	5.63
%+101 Micron in First Precipitator	6.97
%+101 Micron in Last Precipitator	3.62
Total Caustic in First Precipitator (g/L)	0.29
Total Caustic in Last Precipitator (g/L)	0.97
A/TC Ratio in First Precipitator	0.69
A/TC Ratio in Last Precipitator	0.02
g/L Solids in Last Precipitator	4.63

Conclusion

The expense and complications of conducting tests to explore various operating scenarios on an operating plant unit can be formidable. Using predictive chemical process modeling tools can provide a time and cost efficient alternative to such online experimentation. The uses for the dynamic precipitation model which predicts both yield and particle size distribution seem to be almost limitless. Exploiting its dynamic capability, the model can predict the changes which will occur in the process after some change in operating conditions such as a step change in green liquor flow or composition. The model can also predict the impact of plant-wide changes such as changing the total caustic level or a general change in the feed liquor caused by using a variable supply of bauxite. Recently the model has been used as the basis for developing the 1997 operating plan for Point Comfort's precipitation area.

Acknowledgments

The authors wish to thank Raphael Costa and Tom Russell of Point Comfort Operations for their support of the project and invaluable recommendations and Anna Marie Katterson (ATC) who started the coding of the precipitation area.

References

1. J. M. Langa, T. G. Russell, G. A. O'Neill, P. Gacka, V. B. Shah, J. L. Stephenson and J. G. Snyder, "ASPEN Modeling of the Bayer Process," Light Metals 1986, (1986) 169-178.

2. J. L. Stephenson, "Optimization Capability for ASPEN Models of the Bayer Process," Light Metals 1988, (1988) 193-199.

3. T. G. Swansiger, "PRECIP_V2 User's Manual for Computerized Mathematical Modeling of Bayer Cascade Precipitation" (Report No. 6-96-09, Alcoa Technical Center, 1996).

4. J. A. Chapman, P. Winter and G. W. Barton, "Dynamic Simulation of the Bayer Process," Light Metals 1991, (1991) 91-96.

5. W. J. Crama and J. Visser, "Modeling and Computer Simulation of Alumina Trihydrate Precipitation," Light Metals 1994 , (1994) 73-82.

6. J. M. Langa, "Bayer Liquor Heat Capacity and Density" (Report No. 03-85-23, Alcoa Laboratories, 1985).

7. A. D. Randolf and M. A. Larson, Theory of Ind. Eng. Particulate Processes , Academic Press, New York (1971).

8. W. L. McCabe, "Crystal Growth in Aqueous Solutions," Ind. Eng. Chem., 21:1 (1929) 30.

9. J. Scott, "Effect of Seed and Temperature on the Particle Size of Bayer Hydrate," Extractive Metallurgy of Aluminum Volume 1, Alumina , Eds. G. Gerard and P. T. Stroup, American Institute of Mining, Metallurgical, and Petroleum Engineers, Inc., Ann Arbor (1963) 203-218.

10. W. R. King, "Some Studies in Alumina Trihydrate Precipitation Kinetics. Light Metals 1973, (1973) 551-563.

11. C. Misra, "Solubility of Aluminum Trihydroxide (Hydrargillite) in Sodium Hydroxide Solutions," Chemistry and Industry, (1970) 619-623.

12. R. M. Cornell and R. Saunders, "Extent of Agglomeration and Product Toughness," Alcoa of Australia Internal Correspondence (1994).

13. P. G. Groeneweg, "Development of an Al(OH)3 Crystallization Model Based on Population Balance," (Ph.D. thesis, McMaster University, 1980)

14. G. C. Low, "Agglomeration Effects in Aluminum Trihydroxide Precipitation," (Ph.D. thesis, University of Queensland, Brisbane, 1975).

15. D. Ilievsi and E. T. White, "Agglomeration Mechanisms in: $Al(OH)_3$, Crystallization from Caustic Aluminate Solutions", University of Queensland Paper (1995).

16. D.Ilievsi, E. T. White, and M. J. Hounslow, "Agglomeration Mechanism Identification Case Study: $Al(OH)_3$ Agglomeration during Precipitation from Seeded Supersaturated Caustic Aluminate Solutions," University of Queensland Paper (1993).

17. C. Misra, and E. T. White, Kinetics of Crystallization of Aluminum Trihydroxide from Seeded Caustic Aluminate Solutions, Crystallization from Solution: Factors Influencing Size Distribution," Chemical Engineering Progress Symposium Series, AIChE, 67:110 (1971) 53-65.

18. C. Misra, private communication, 1984.

19. O. Molerus, "Stochastiches Modell der Gleichgewichtsichtung," Chemie-Ing-Techn, 39, (1967), 792-796.

20. J. Ohkawa, T. Tsuneizumi and T. Hirao, "Technology of Controlling Soda Pick-up in Alumina Trihydrate Precipitation," Light Metals 1985, (1985) 345-366.

21. J. F. Ralphe, "Global Relation for Fixed Soda," Alcoa Technical Memo (1996).

22. Mitchell and Gauthier Associates, Inc., Advanced Continuous Simulation Language (ACSL) Reference Manual., Edition 11.1 (1995) Concord, MA.

Recommended Reading

Chen, C., et al. Bayer process simulation by Aspen (1983, pp. 295–312).

Hardin, M.B. On-line multivariable control for digestion AIC analysis (1991, pp. 45–50).

Jonas, R.K. Application and benefits of advanced control to alumna refining (2004, pp. 43–49).

Leclerc, A., et al. Influence of Bayer liquor composition on the measurement of slurry velocity using an electrochemical flowmeter (2003, pp. 99–103).

McIntosh, P. Optimum control of bauxite charge to high temperature digestion units at QAL. (1984, pp. 21–38).

Misra, C., and V. Soi. Development of software for Bayer process alumina plants (1997, pp. 81–88).

Muller, T.B., and T.L. Johnson. Simulation of mass, heat, and particulate balances in the Bayer precipitation (1979, pp. 3–29).

Wind, S., et al. Dynamic simulation of gas suspension calciner (GSC) for alumina (2011, pp. 137–143).